Analyst

Accepted Manuscript

ROYAL SOCIETY OF CHEMISTRY

www.rsc.org/analyst

Cite this: DOI: 10.1039/c0xx00000x

www.rsc.org/xxxxxx

ARTICLE TYPE

High specific detection of Osteopontin with three-dimension copolymer layers support based on electrochemical impedance spectroscopy

Hongxia Chen[a], Qiaohan Mei[a], Shengsong Jia[a], Kwangnak Koh[b], Keming Wang[c],*, Xinjian Liu[d],*

Received (in XXX, XXX) Xth XXXXXXXXX 20XX, Accepted Xth XXXXXXXXX 20XX

DOI: 10.1039/b000000x

Tumor marker detection is essential to therapy efficiency of early stage tumor and evaluation of disease progression. Osteopontin (OPN) is supposed to be closely related to several kinds of tumors. We describe here a label-free electrochemical detection of OPN based on the specific reaction between OPN and its relevant antibody. An artificial three-dimension (3D) scaffold structure consisting of 11-mercapto undecanoic acid/6-mercapto-1-hexanol, dextran amino and synthetic peptides was designed as a substrate for immobilization of antibody. This substrate was characterized with cyclic voltammetry, atomic force microscopy and Fourier transform infrared reflection spectroscopy. Antibody immobilization and OPN detection were conducted with electrochemical impedance spectroscopy (EIS). The low limit of detection is 0.17 nM. The concentration of cancer risk (5.77 nM) can be detected selectively with high EIS signal. The fabricated 3D OPN sensor is proposed for application in clinical analysis.

[a]*Laboratory of Biosensing Technology, School of Life Sciences, Shanghai University, Shanghai 200444, China*
[b]*Department of Applied Nanoscience, Pusan National University, Miryang, 627-706, Republic of Korea*
[c]*Department of Oncology, The Second Affiliated Hospital of Nanjing Medical University, Nanjing 210011, China*
[d]*Department of Biochemistry and State Key Laboratory of Pharmaceutical Biotechnology, Nanjing University, Nanjing 210093, China*
**Corresponding authors. Fax: +86 25 58509994 (K. Wang), +86 25 83592510 (X Liu). E-mail addresses: wkmys@sohu.com (K. Wang), liuxj@nju.edu.cn (X. Liu)*

1. Introduction

In 1979, Osteopontin (OPN) was first reported by Senger[1] and described as a phosphoprotein which regulated the tumor metastasis. OPN is involved in various tumorous activities such as tumor angiogenesis[2], invasion, adhesion, migration[3-6], evading recognition/ destroy from immune system and inhibition of tumor apoptosis. Its expression in the healthy heart and blood vessels is very low, but consistently up-regulated in increasing kinds of cancer diseases like laryngocarcinoma, gastric carcinoma, breast cancer, esophagus cancer, renal carcinoma, colorectal cancer and uterine cervical cancer[7-9]. Besides cancers, other diseases are also related with OPN expression. Development of granuloma in tissues and glomerulonephritis in the kidney results from upregulation of OPN expression[10]. In recent years' study, OPN is defined as a significant role in the formation and calcification of atherosclerotic plaques[11]. Pedersen et al. have also demonstrated a notable role of OPN in development and progression of plaque in uraemia[12]. Thus, OPN has attracted considerable attention as its potential to be a diagnosis marker and therapeutic target in several disease processes. Since then, some methods have been developed for the detection of OPN like enzyme-linked immunosorbent assay (ELISA) which may not be very sensitive[13]. And till now, ELISA is still the most common method used in clinical detection. However, as ELISA is highly time-consuming and expensive, building a novel, sensitive and convenient approach is essential.

Electrochemical immunosensors have displayed many advantages like simplicity, low detection limit and easy integration into miniaturized systems in the field of clinical diagnostics and drug discovery[14]. In electrochemical immunosensors, the immunological compounds (antibody or antigen) are usually indirectly immobilized on an electrode (gold electrode or others). A variety of specific molecules are applied to linker between electrodes and antibodies. Dextran amine (DA) is one of the most common linkers which are widely used to immobilize proteins[15, 16]. It is a linear polymer based on 1,6-linked glucose units and abundant in amino groups. There are two advantages of the DA multilayer. First it can decrease the possibility of protein denaturation and minimize nonspecific binding of ligands to the sensor surface, on account of an effective barrier between biomolecules and the gold substrate. Another advantage is that DA can provide multilayer of amino sites for substrate immobilization acted as a three-dimension (3D) scaffold and more binding capacity than other two-dimension linkers, because the DA matrix has numerous amino group functionalities along its backbone[17]. Many kinds of 3D substrates have been applied in the biosensors, but the cost and complexity of construction process are the most unintelligible problems[18-20]. Chen et al.[18] published a novel 3D sensor based on kinds of nanomaterial with a long procedure and rigorous condition. DA structure can be made via common covalent reaction and mild condition. So except the two advantages mentioned above, DA applied in biosensor can also economize time and resource expense.

The Fc region of antibody is an amine-rich region and the direct linkage between COOH functional groups of SAM and Ab can be used for surface immobilization. However, the direct reaction between protein's carboxyl and DA's amino probably destroys the active region of protein and this linking method can't guarantee the most effective orientation of antibody which depends on antibody's subtypes[21]. So, many scientists are trying hard to develop a molecule that specifically binds to non-active region of protein. Fc region is the non-active region of antibody and Fab region can specifically bind to antigen. Carbonell et al. have identified HWRGWV as a new hexamer peptide which selectively binds to the Fc region of IgG[22-25]. And the binding affinity of the short peptide with IgG is ~10^5 M^{-1}, which is lower than that for protein A, the conventional immobilizing molecule[26]. These features make HWRGWV become a viable alternative for antibody immobilization to other systems based on protein A/G.

Herein, we report a label-free 3D scaffold electrochemical immunosensor for OPN detection in this paper. Electrochemical impedance spectroscopy (EIS) is chosen as the major method in this study. EIS is a simple, sensitive and convenient technique which provides electrical information in capacitance, reactance and resistance changes. Due to its ability to probe into the interfacial properties of an electrode surface, EIS has been increasingly applied to the transduction of biosensing events at the electrode surface [27-29]. As shown in Fig.1, OPN's antibody (anti-OPN) is immobilized on the surface of a gold electrode which is pre-modified with 11-mercapto undecanoic acid/6-mercapto-1-hexanol (MUA/MCH), DA and acetylated-HWRGWVA (HA-7) step by step. MUA is used to immobilize DA. MCH here is a blocking agent which not only backfills the gold disk so as to resist nonspecific binding and obtain well aligned MUA monolayers, but also retains appropriate space for the following modification and adsorption. DA acts as a 3D scaffold which provides a considerable space and adequate sites for HA-7 and antibody immobilization. HA-7 ensures the orientation and activity of antibody. The phenomenon of every step in the experiments can be characterized by increase of impedance value displayed by the electrochemistry instrument. All these advantages make OPN be detected sensitively and conveniently.

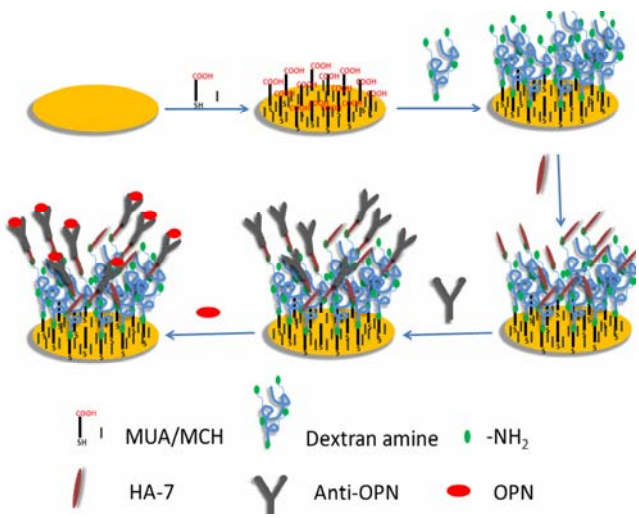

Figure 1 Experimental scheme for detection of OPN on Au surface.

2. Experimental

2.1 Materials and chemicals

Ethanolamine, 6-mercapto-1-hexanol (MCH), 11-mercapto undecanoic acid (MUA), 1-ethyl-3-(3-dimethylaminopropyl) carbodiimide hydrochloride (EDC), N-hydroxy succinimide (NHS), N,N-Dimethylformamide (DMF, anhydrous), potassium ferricyanide buffer solution, phosphate-buffered saline (PBS, 150 mM, 1M NaCl, pH 7.4) and bovin serum albumin (BSA) were purchased from Sigma-Aldrich (St. Louis, MO). O-(7-acabenzotriazo(-1-yl))-N,N,N',N'-tetramethyluronium hexafluorophosphate (HATU) and N,N-diisopropylethylamine (DIPEA) were purchased from Sinopharm Chemical Reagent Co., Ltd. (Shanghai, PR China). Dextran amine (DA) was purchased from Life Technologies Corporation (Eugene, USA). Anti-human osteopontin (Anti-OPN) was purchased from Immuno-Biological Laboratories Co., Ltd. (Fujioka, Japan). Recombinant human osteopontin (OPN, 44 kDa) was ordered from Sino Biological Inc. (Beijing, China). Acetylated-HWRGWVA (HA-7) was synthesized by Shanghai Sangon Biological Engineering Technology (Shanghai, China). Potassium ferricyanide buffer solution was dissolved in PBS and stored at 4 ℃ before use. MUA&MCH mixed solution was dissolved in ethanol. HA-7 was dissolved in DMF and distilled water used in this work was from a Millipore Milli-Q water purification system.

2.2 Formation of supporting self-assembly monolayer (SAM)

Before functionalization, gold electrode (2 mm in diameter) was firstly abraded with silicon carbide paper and then polished to a mirror-like surface with alumina powder (Al_2O_3). Residual alumina powder was removed by sonicating the electrode for 5 min in ethanol and distilled water, respectively. Then the electrode was soaked in piranha solution (98% H_2SO_4: 30% H_2O_2=3: 1) for 5 min to eliminate the adsorbed material. After being rinsed with distilled water, the electrode was further electrochemically cleaned to remove any remaining impurities in 0.5 M H_2SO_4. After being dried with nitrogen, the electrode was immediately immersed in MUA&MCH mixed solution (2.5 mM : 7.5 mM) overnight. Then washed with ethanol and distilled and dried with nitrogen, the electrode was prepared well for next operation.

2.3 Preparation of a three-dimension (3D) modified electrode

The modified electrode was immersed in 1:1 (v/v) EDC (400 mM) & NHS (100 mM) mixed solution for 20 min to activate the end carboxyl of MUA molecule. After activation, the electrode was incubated with dextran amine (0.1 mg/mL, dissolved in distilled water) for 15 min. The rich amino from dextran amine should capture the activated carboxyl through covalent reaction. In order to block the nonspecific binding of other molecules onto the activated carboxyl, the gold electrode was treated with 10μL 1 M ethanolamine (pH 8.5).

Acetylated-HWRGWVA (HA-7, 0.5 mg/mL) peptides were immobilized on the electrode via covalent amide bonds by the reaction of the peptides' carboxylate groups with amino of dextran amine. The electrode was immersed in an anhydrous DMF solution containing HA-7 (0.5 mg/mL) and HATU (3.8 mg/mL), followed by addition of DIPEA (2.58 μL/mL). The incubation period last 12 h at room temperature under a nitrogen atmosphere. Finally, the surfaces were rinsed with DMF and abundant Milli-Q water to remove unreacted and physically adsorbed molecules, and then dried under a nitrogen flow to achieve a 3D modified electrode.

2.4 Antibody immobilization and detection of OPN

Anti-OPN was used as a capture protein to immobilize on the 3D modified electrode. It was dissolved in PBS. PBS here with addition of 1 M NaCl can greatly decrease nonspecific electrostatic binding of BSA[27]. The electrode was incubated with the Anti-OPN solution (10 μg/mL) for 3 h and then washed with PBS gently. OPN with six different concentrations in a range of 2.27, 3.41, 5.68, 9.08, 13.62, 20.43 nM was in sequence incubated with electrode for 1 h at 37 ℃ and followed by rinsing with PBS. BSA with the same molar concentration was chosen as the control group. A control experiment that antibody was directly immobilized on the MUA/MCH monolayer was also conducted to make a legible comparison.

2.5 Surface characterization of 3D modified electrode

Atomic force microscopy (AFM) was employed here to show a visual status of gold surface after immobilization of 3D structure. The gold surface was prepared by a sputter coater/carbon evaporator (Q150RS, Quorum Technologies, Kent, UK). Gold is sputtered on a micro cover glass (18×18 mm, thickness 0.12-0.17 mm, Matsunami, Japan) under a sputter current of 40 mA for 120 s. The measurements were conducted on an AFM instrument (Agilent 5500, Santa Clara, CA). AFM images were collected at a scan rate of 0.5-1 Hz in tapping mode with a resolution of 512×512 pixels. AFM tips with resonant frequency in the range 160-260 kHz were used. Bare gold, MUA, DA and peptide images should be collected respectively.

After immobilization of dextran amine, the whole amount of amino should be abundant on gold surface. For characterization the chemical ingredients of 3D structure, Fourier transform infrared reflection spectroscopy (FTIR, VERTEX 70, Bruker Optics, Ettlingen, Germany) spectra were measured with a resolution of 2 cm^{-1}. A p-polarized IR beam was used as the light source.

2.6 Electrochemistry measurements of stepwise reactions on the gold surface

EIS and cyclic voltammetry (CV) were carried out on a Metrohm electrochemical analyzer (Metrohm Autolab B.V., the Netherlands) in 0.01 M PBS (pH 7.2) containing 0.1 M KCl and 5 mM $[Fe(CN)6]^{3-/4-}$. A three-electrode system consisting of the modified gold electrode (diameter is 3 mm), a saturated calomel reference electrode (SCE) and a platinum counter electrode was used for all the electrochemical measurements. The whole process reacted on the electrode was measured by EIS and CV. The electrode after every step of modification must be used immediately in case of the denaturation of biomolecules on electrode.

3. Results and discussion

3.1 Characterization of 3D scaffold on gold electrode

After three-step incubations, 3D scaffold was fabricated on the electrode. CV was first here employed to display the change of electrochemical property on gold surface. As shown in Fig.2, the electrochemical probe, $[Fe(CN)_6]^{3-/4-}$, gives a pair of stable and

unambiguous peaks at the bare gold electrode (curve a, black line). In Table 1. I_{pa}, E_{pa} and E_{pc} denote anodic peak current, anodic peak potential and cathodic peak potential. The peak separation (ΔE_p) is 68 mv suggesting a fast and reversible electron transfer process. After the monolayer of MUA/MCH is assembled on the electrode surface, a significant increase in the peak separation (187 mv) and the decrease of peak currents can be observed (curve b, red line), demonstrating that MUA/MCH has been self-assembled on the electrode surface. After the further incubation with DA and peptides in sequence, the redox peak separation has continued to be increased (ΔEp=193 mV, curve c, blue line and ΔEp=258 mV, curve d, cyan line). The average peak current after peptide immobilization is decreased to 87.92 μA (curve d, cyan line) and compared with that 140.08 μA (curve a, black line) for the bare and 89.69 μA (curve b, red line) for the MUA/MCH modified electrode. The peak current after DA immobilization is increased slightly to be 103.42 μA (curve c, blue line) compared with that 89.69 μA (curve b, red line) for the MUA/MCH modified electrode. This may be causes by the positive electricity of DA's abundant amino that would accelerate the electron transferring through electrode surface.

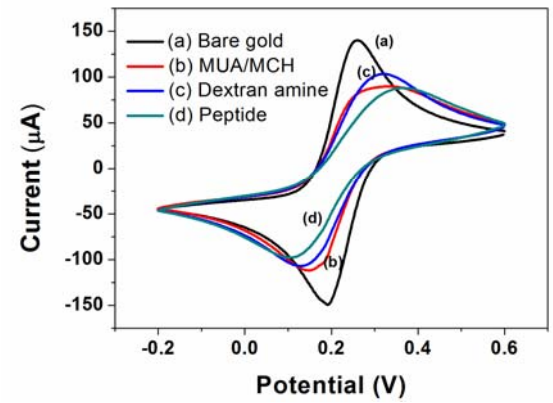

Figure 2 Cyclic voltammograms obtained at (a) the bare gold electrode, (b) MUA/MCH modified gold electrode, (c) dextran amine modified electrode and (d) peptide modified electrode. Scan rate: 100 mV/s.

Table1. The peak values in CV graph

Curve	a	b	c	d
***I*pa (μA)**	140.08	89.69	103.42	87.92
Epc(mv)	193	147	128	106
Epa(mv)	261	334	321	364
ΔEp (mv)	68	187	193	258

To enhance the effectiveness of the design, AFM has been employed to display the surface geometry and FTIR has been used to measure the element composition of electrode surface. As shown in Fig.3 (A) and (B), bare gold surface's average amplitude is about 3.5 nm and after modification with DA (Fig.3 (C) and (D)), amplitude is increased to nearly 8 nm, which confirmed the DA as a polymer is immobilized on the gold surface. As shown in Fig.3 (D), DA on the surface is not very tightness. Cavities that show low amplitude in the line profile can be found and easy to accommodate other molecules. DA contains rich amine groups to interact with the following peptides. After modification with the peptide HA-7, the line profile in Fig.3 (F) becomes close which displays an abundant content of peptide immobilized on DA. The strip of peptide is also shown in Fig.3 (E) directly.

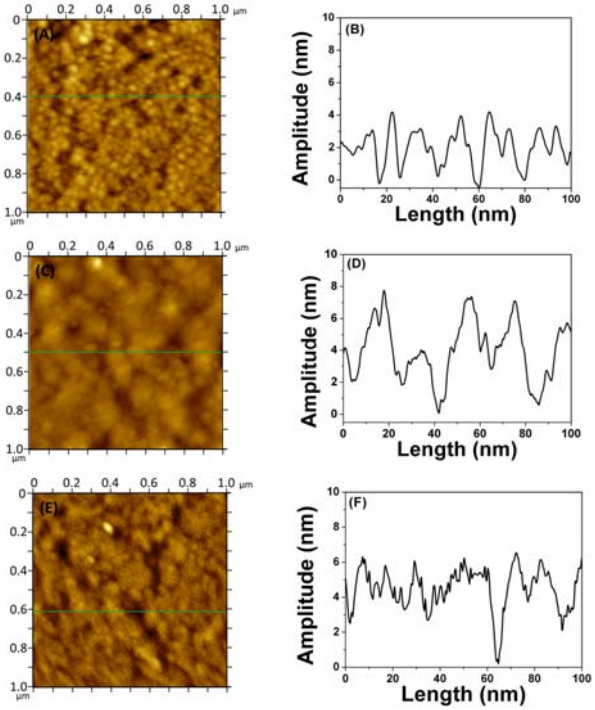

Figure 3 AFM images and line profiles of the bare gold film (A and B), DA modified gold surface (C and D) and the peptide HA-7 modified gold surface (E and F).

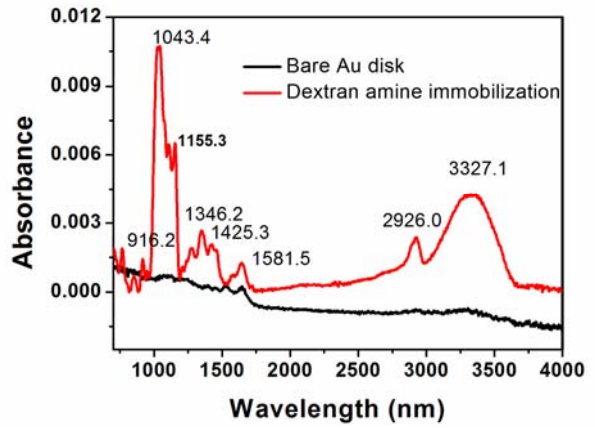

Figure 4 FTIR spectra of bare Au and DA modified Au surface.

Also, in Fig.4, the typical FTIR spectra of the dextran layer on the gold surface can be observed. The red line illustrates DA's IR spectra and the black line is the control bare gold disk. The bands at 2926.0, 1043.4, and 916.2 cm^{-1} represent the presence of C–H bonds, C–O bonds and the α-glucopyranose ring, respectively which reveal the main body of DA molecule. We may also observ the bands at 3327 cm^{-1}, 1581.5 cm^{-1} and 1155.3 cm^{-1} which are attributed to the N-H stretch mode, the –C (=O)-N-H secondary amine bond, and the antisymmetric stretch of the C-N-C secondary amine moiety, respectively. These bands at 1346.2 and 1425.3 cm^{-1} are attributed to the $–NH_2$ of bending mode of free

amino groups[30]. Combining FTIR, AFM and CV results, it is clear that DA and peptide HA-7 have been successfully constructed on the gold electrode surface and is ready to capture antibody.

3.2 Characterization of antibody immobilization

As one of the most commonly used approach, EIS is here to characterize the immobilization of antibody. As shown in Fig.5 (A), curve a, the EIS response is nearly a straight line at the bare gold electrode, which implies a very low electron transfer resistance (R_{et}). After the final modification of peptides, a high R_{et} can be evidently observed (Fig.5 (A), curve b). This indicates that peptides have been immobilized on the electrode. Then, after incubation with antibody, a higher increase of the R_{et} is induced (Fig.5 (A), curve c) which is attributed to the oriented interaction between peptides and antibody. For comparing and analyzing the advantages of 3D scaffold, we have also conducted experiments which make antibody to be directly immobilized on MUA/MCH monolayer[20]. The result is shown in Fig.5 (B). The differential of R_{et} between MUA/MCH and antibody (Fig.5 (B), curve b and c) is much smaller than that between peptide and antibody (Fig.5 (A), curve b and c). This result clearly shows the high capacity of 3D scaffold.

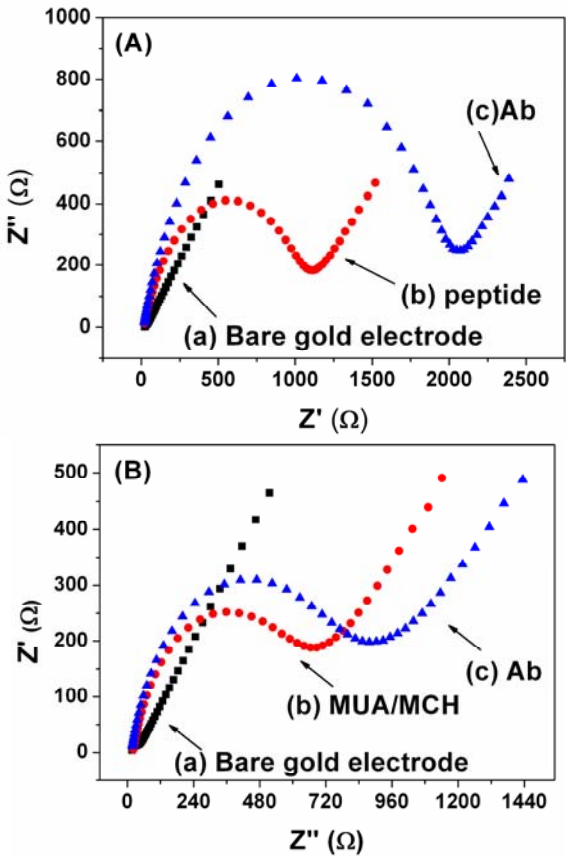

Figure 5 Nyquist plots of electrochemical impedance spectra of modified electrode stepwise on (A) 3D scaffold structure and (B) MUA/MCH monolayer. Bias potential: 0.224 V; Amplitude: 5 mv; Frequency range: 0.1 Hz to 100 kHz.

3.3 Detection of OPN

EIS has also been used to conduct the OPN detection measurement. EIS data are fit to an Equivalent Electrical Circuit (EEC) to extract quantitative information about the processes occurring at the electrode surface. The calculation principle is based on the Randle's equivalent circuit using a constant phase element (CPE) shown in Fig.6 (A) insert. A Warburg impedance (W) which models linear diffusion toward the electrode surface. R_{et} can be calculated with a customized software called Nova (Metrohm Autolab B.V., the Netherlands), which is related with the surface change of electrode [29, 31].

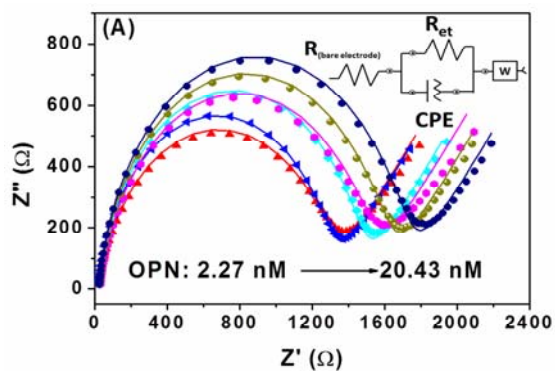

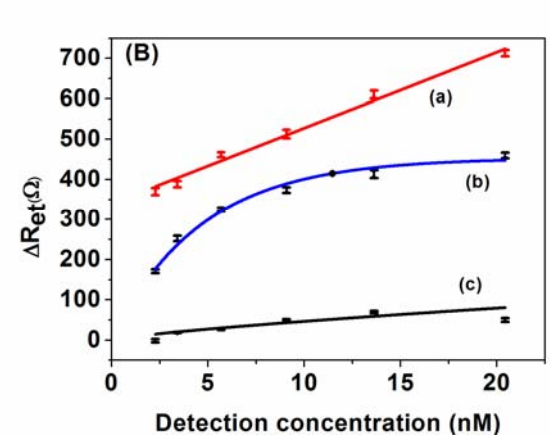

Figure 6 (A) Nyquist plots of electrochemical impedance spectra obtain after Ab adsorption （black square）and at different concentrations of OPN (2.27 nM, 3.41 nM, 5.68 nM, 9.08 nM, 13.62 nM and 20.43 nM) on 3D scaffold structure (symbol series is the measurement data and line series is the EIS simulation results). Insert: The Randle's equivalent circuit using a constant phase element; (B) Relationship between Ret and the antigen concentration at three different conditions ((a): OPN on 3D structure, (b): OPN on MUA/MCH monolayer, (c): BSA as control on 3D structure).

As shown in Fig.6 (A), symbol series are the measurement data observed on the 3D scaffold structure and line series are the EIS simulated results according measurement data. The simulation data shown in the solid line are well consistent with the experimental data. With the rise of OPN concentration, R_{et} is increased evidently. Fig.6 (B) shows that the differential of R_{et} (ΔR_{et}) that OPN is detected with 3D scaffold increases larger than that detected with monolayer at every concentration. Even at the lowest concentration 2.27 nM, the increase of R_{et} is about 375 Ω on 3D scaffold structure which is larger than that 152 Ω on MUA/MCH monolayer. As 5.77 nM is a clinical concentration limit which implies cancer risk[32], the detection effect at this

concentration shall be a key indicator to estimate the sensor performance. Judged by both line (a) and (b), the ΔR_{et} at the concentration of 5.68 nM, is beyond 300 Ω. Moreover, 3D scaffold shows higher reaction extent that ΔR_{et} is almost 450 Ω than monolayer with ΔR_{et}, 300 Ω. OPN detection using 3D scaffold structure shows good linearity from 2.27 to 20.43 nM with R^2 =0.98. The control group was injected with bovine serum albumin (BSA) solution with the corresponding concentrations. As shown in Fig.6 (B), line (c), after incubation with BSA at different concentration, the ΔR_{et} almost keeps at the zero level for the control group even in the higher concentration. Therefore, the increase in the SPR signal obtained for the experimental group can definitely denote the specific interaction of the antibody and OPN. The whole trends of the experimental group and the control group verified that OPN could be detected spcifictly. The low limit of detection (LLD) was calculated as 0.17 nM (LLD = 3.3 × standard deviation / slope). These results also show that 3D scaffold structure is more sensitive and can provide higher signal than monolayer structure, which may own to the high capacity and good Ab orientation at 3D scaffold structure.

4. Conclusions

In summary, a convenient and label-free biosensor fabricated with high-capacity 3D scaffold structure for detection of tumor marker OPN has been developed. This biosensor provides more protein capacity and the cancer risk (OPN concentration 5.77 nM) can be detected with a higher EIS signal than normal monolayer sensor. In addition, the potential of clinical diagnosis application may also be supported by the good specificity of this biosensor. This biosensor not only shows a good performance in OPN detection, but also provides a novel platform for other tumor marker detection and may contribute to the development of early tumor diagnosis and therapy.

Acknowledgement

This work is supported by the National Natural Science Foundation of China (Grant Nos. 61275085, 31100560).

References

1. D. R. Senger, D. F. Wirth and R. O. Hynes, *Cell*, 1979, **16**, 885-893.
2. H. Tang, J. Wang, F. Bai, L. Hong, J. Liang, J. Gao, H. Zhai, M. Lan, F. Zhang and K. Wu, *Biochem. Cell B.*, 2007, **85**, 103-110.
3. D. Weismann, J. Briese, J. Niemann, M. Grüneberger, P. Adam, S. Hahner, S. Johanssen, W. Liu, S. Ezzat and W. Saeger, *J. Pathol.*, 2009, **218**, 232-240.
4. Y. J. Chen, Y. Y. Wei, H. T. Chen, Y. C. Fong, C. J. Hsu, C. H. Tsai, H. C. Hsu, S. H. Liu and C. H. Tang, *J.Cell Physiol.*, 2009, **221**, 98-108.
5. L. Shevde, S. Das, D. Clark and R. Samant, *Curr. Mol. Med.*, 2010, **10**, 71-81.
6. B. S. Sun, Q. Z. Dong, Q. H. Ye, H. J. Sun, H. L. Jia, X. Q. Zhu, D. Y. Liu, J. Chen, Q. Xue and H. J. Zhou, *Hepatology*, 2008, **48**, 1834-1842.
7. X. Lu and L. G. MO, *Med. Rec.*, 2007, **19**, 1441-1443.
8. M. Higashiyama and M. Yutaka Shimada, *Ann. Surg. Oncol.*, 2007, **14**, 3419-3427.
9. W. Likui, W. Hong and Z. Shuwen, *J. Gastrointest. Surg.*, 2010, **14**, 74-81.
10. I. Carlson, K. Tognazzi, E. J. Manseau, H. F. Dvorak and L. F.Brown, *Lab. Invest.*, 1997, **77**, 103-108.
11. C. Foresta, G. Strapazzon, L. De Toni, F. Fabris, F. Grego, G. Gerosa, S. Vettore and A. Garolla, *J. Thromb. Haemost.*, 2013, **11**, 357-365.
12. X. Zhang, A. Eirin, A. Lerman and L. O. Lerman, *Cardiovasc. Res.*, 2013, **98**, 332-333.
13. S. I. Funano, T. G. Henares, M. Kurata, K. Sueyoshi, T. Endo and H. Hisamoto, *Anal. Biochem.*, 2013,**440**,137-141.
14. M. Yang, X. Yi, J. Wang and F. Zhou, *Analyst*, 2014, **139**, 1814-1825.
15. G. Zeder-Lutz, S. Renau-Ferrer, V. Aguié-Béghin, H. Rakotoarivonina, B. Chabbert, D. Altschuh and C. Rémond, *Analyst*, 2013, **138**, 6889-6899.
16. S.C.B Gopinath and P.K.R. Kumar, *Analyst*, 2014, DOI:10.1039/c3an02052e.
17. S. Paynter and D. A. Russell, *Anal. Biochem.*, 2002, **309**, 85-95.
18. Y. Chen, C. Wu, J.J. Tasi and G. Wang, *Int. J. Nanomed.*, 2012, **7**, 133-140.
19. C.C. Tsai, G.J. Wang, *J. Electrochem. Soc.*, 2013, **160**, B1-B5.
20. T. Bertok, A. Sediva, A. Vikartovska, J. Tkac, *Int. J. Electrochem. Sci.*, 2014, **9**, 890-900.
21. J. Zhou, H.K. Tsao, Y.J. Sheng, S. Jiang, *J. Chem. Physics.*, 2004, **121**,1050-1057.
22. A. D. Naik, S. Menegatti, P. V. Gurgel and R. G. Carbonell, *J. Chromatogr. A*, 2011, **1218**, 1691-1700.
23. H. Yang, P. V. Gurgel and R. G. Carbonell, *J. Pept. Res.*, 2005, **66**, 120-137.
24. H. Yang, P. V. Gurgel, D. K. Williams, B. G. Bobay, J. Cavanagh, D. C. Muddiman and R. G. Carbonell, *J. Mol. Recognit.*, 2010, **23**, 271-282.
25. Z. Liu, P. V. Gurgel and R. G. Carbonell, *J. Chromatogr. A*, 2011, **1218**, 8344-8352.
26. H. Yang, P. V. Gurgel and R. G. Carbonell, *J. Chromatogr. A*, 2009, **1216**, 910-918.
27. F. Lisdat and D. Schäfer, *Anal. Bioanal. Chem.*, 2008, **391**, 1555-1567.
28. A.B. Bandarenka, *Analyst*, 2013, **138**, 5540-5554.
29. M.A. MacDonald, H.A. Andreas, *Electrochimica Acta,* 2014, **129,** 290–299.
30. V. Ayala, A. P. Herrera, M. Latorre-Esteves, M. Torres-Lugo and C. Rinaldi, *J. Nanopart. Res.*, 2013, **15**, 1-14.
31. D. Chen, M. Shen, Y. Cao, B. Bo, Z. Chen, Y. Shu and G. Li, *Electrochem.Commun.*, 2013, **27**, 38-41.
32. J.-H. Kim, S. J. Skates, T. Uede, K. K. Wong, J. O. Schorge, C. M. Feltmate, R. S. Berkowitz, D. W. Cramer and S. C. Mok, *J. Am. Med. Assoc.*, 2002, **287**, 1671-1679.

Graphic Abstract

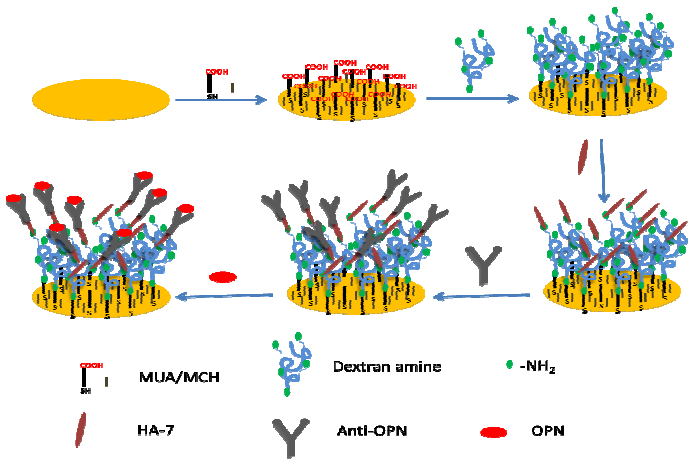

Specific detection of Osteopontin with three-dimension copolymer layers support.